ORGANOMETALLICS

Article

Cite This: *Organometallics* 2018, 37, 3863−3873

pubs.acs.org/Organometallics

Tetramethylcyclopentadienyl Ligands Allow Isolation of Ln(II) Ions across the Lanthanide Series in [K(2.2.2-cryptand)][$(C_5Me_4H)_3Ln$] Complexes

Tener F. Jenkins, David H. Woen, Luke N. Mohanam, Joseph W. Ziller, Filipp Furche,* and William J. Evans*

Department of Chemistry, University of California, Irvine, California 92697-2025, United States

Supporting Information

ABSTRACT: Although previous studies of the stabilization of Ln(II) ions across the lanthanide series have relied on Me_3Si-substituted cyclopentadienyl ligands, we now find surprisingly that these ions can also exist surrounded by three tetramethylcyclopentadienyl ligands. Reduction of the $4f^n$ Ln(III) complexes, $Cp^{tet}{}_3Ln$ (Cp^{tet} = C_5Me_4H) using potassium graphite in the presence of 2.2.2-cryptand (crypt) produces the Ln(II) complexes, [K(crypt)][$Cp^{tet}{}_3Ln$] for Ln = La, Ce, Pr, Nd, Sm, Gd, Tb, and Dy, all of which were characterized by X-ray crystallography. These complexes display intense absorptions in the UV−visible−near IR region that are red-shifted compared to those of previously characterized $(Cp'_3Ln)^{1-}$ complexes (Cp′ = $C_5H_4SiMe_3$). The thermal stability of these new Ln(II) complexes decreases with the size of the metal.

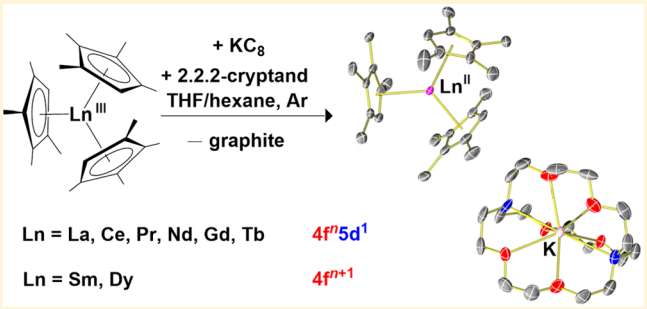

INTRODUCTION

In recent years, the range of oxidation states available to the rare-earth metals in crystallographically characterizable molecular complexes available for reactivity in solution has greatly expanded.[1,2] Up until 2001, it was thought that only six lanthanides could form crystallographically characterizable molecular complexes of Ln(II) ions in solution: Eu, Yb, Sm, Tm, Dy, and Nd.[3−6] These complexes could be made by reduction of $4f^n$ Ln(III) precursors and formed Ln(II) ions with $4f^{n+1}$ electron configurations as expected. However, it is now known that yttrium and all of the lanthanides (except Pm which was not studied due to its radioactivity) can form isolable molecular complexes of Ln(II) ions if reductions are done in the proper coordination environment.[7−12] Specifically, reduction of tris(cyclopentadienyl) complexes with silyl-substituted ligands $C_5H_3(SiMe_3)_2$ (Cp″)[7,8] and $C_5H_4SiMe_3$ (Cp′)[9−12] provided access to Ln(II) ions across the series, as shown in eq 1.[1,2] This was also extended to the actinides, Th,[13]

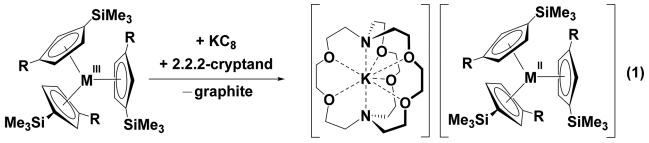

R = H; M = Y, La, Ce, Pr, Nd, Sm, Gd, Tb, Dy, Ho, Er, Tm, Lu, U
R = $SiMe_3$; M = La, Ce, Pr, Nd, Th, U, Np, Pu

U,[14,15] Pu,[16] and Np.[17] Examples of complexes of new Ln(II) ions are also known with $C_5H_3(CMe_3)_2$ (Cp^{tt})[18,19] and $C_5H_2(CMe_3)_3$ (Cp^{ttt})[20,21] and the tris(aryloxide) mesitylene ligand, $[(^{Ad,Me}ArO)_3mes]^{3-}$.[22,23] Extensive crystallographic, spectroscopic, magnetic, and density functional theory (DFT) studies showed that the new Ln(II) ions in the tris(cyclopentadienyl) environments adopted $4f^n5d^1$ electron configurations.[1,7−12,23−26] This could be rationalized by the crystal field splitting of a tris(cyclopentadienyl) coordination environment, which puts a $5d_{z^2}$ orbital comparable in energy to the 4f orbitals.[27−32]

A comparison of the rare-earth metals in the [K(crypt)][Cp'_3Ln] series (crypt = 2.2.2-cryptand) revealed that Ln(II) ions could be grouped into three categories.[10] Sm, Eu, Tm, and Yb form complexes of traditional Ln(II) ions with $4f^{n+1}$ electron configurations. For Ln = Nd and Dy, the [K(crypt)][Cp'_3Ln] complexes have $4f^n5d^1$ configurations, but in other ligand environments, the metals form $4f^{n+1}$ Ln(II) ions. These are designated as configurational crossover ions. Nd(II) and Pr(II) are known to be configurational crossover ions in the solid state iodides, LnI_2.[33,34] The third category contains the rest of the lanthanide metals which have $4f^n5d^1$ configurations and Y(II) which is a $4d^1$ ion.

After the first Y(II) complex, $(Cp'_3Y)^{1-}$, was isolated,[11] the importance of the ligand system was examined by studying the reductions of $Cp_3Y(THF)$ (Cp = C_5H_5), $Cp^{Me}{}_3Y(THF)$ (Cp^{Me} = C_5H_4Me), and Cp''_3Y.[25] In each case, the reduction product

Received: August 2, 2018
Published: October 18, 2018

DOI: 10.1021/acs.organomet.8b00557
Organometallics 2018, 37, 3863−3873

was examined in solution by EPR spectroscopy.[9,11] Each EPR spectrum showed a two-line hyperfine pattern, which is consistent with the interaction of an unpaired electron with the 100% naturally abundant ^{89}Y (I = 1/2) nucleus. However, none of these ligand systems gave isolable Y(II) complexes as found in the reduction of Cp'_3Y. Comparison of the hyperfine coupling constants, Table 1, of these tris(cyclopentadienyl)

Table 1. Comparison of EPR Parameters of Reduction Products of YL_3 Complexes (L = Ligand)

compound reduced	g_{iso}	A_{iso} (G)
Cp''_3Y[25]	1.9908	36.1
Cp'_3Y[25]	1.991	36.6
$Cp_3Y(THF)$[25]	1.9905	42.8
$Cp^{Me}_3Y(THF)$[25]	1.9903	46.9
$Y(NR_2)_3$[35]	1.976	110

complexes along with that of the solution reduction product of $Y(NR_2)_3$ (R = $SiMe_3$), a system that also did not give an isolable Y(II) complex,[35] suggested an explanation for the observed results. The more unstable complexes had larger hyperfine coupling constants. These larger hyperfine coupling constants observed in the reductions of $Y(NR_2)_3$, Cp^{Me}_3Y, and Cp_3Y compared to Cp'_3Y suggested that the NR_2, Cp^{Me}, and Cp ligands were more electron donating than Cp′ in this yttrium system and made the Y(II) complex too electron-rich to be isolated. These results were consistent with data obtained on electrochemical analysis of $(C_5R_5)_2ZrCl_2$ complexes,[36] as well as studies by Lappert that showed that it was more difficult to reduce $[C_5H_3(CMe_3)_2]_3La$ than $[C_5H_3(SiMe_3)_2]_3La$.[19] The instability of Cp''_3Y is attributed to the steric crowding in this complex with the large ligand and the small metal.[37,38]

However, the recent isolation of +2 ions in complexes of NR_2 (R = $SiMe_3$) ligands suggested that strongly donating ligands could also provide these new ions. Specifically, amide ligands were used to isolate the first crystallographically characterizable complex of a +2 ion of the smallest rare-earth metal, scandium, as well as the lanthanides, Ln = Nd, Gd, Tb, Dy, Ho, and Er, in the compounds $[M(chelate)][Ln(NR_2)_3]$ (M = K, Rb; chelate = 18-crown-6 and crypt; R = $SiMe_3$).[39,40] Consequently, we have examined the reduction of Cp^{tet}_3Ln complexes (Cp^{tet} = C_5Me_4H). These complexes were not examined earlier[25] because it was assumed that the Cp^{tet} ligand was too electron donating to form stable complexes. We report here that the $(Cp^{tet}_3)^{3-}$ ligand set provides an entire new *series* of Ln(II) complexes that allows evaluation of the three categories of Ln(II) complexes as a function of metal.

RESULTS

Yttrium. The reduction of Cp^{tet}_3Y, **1-Y**, in THF using KC_8 in the presence of crypt produced a dark blue solution, **2-Y**, that decomposed to an orange solution within minutes even at −35 °C. In order to obtain EPR data on the reduction product, the reaction was performed in an EPR tube at −78 °C.

The EPR spectrum, Figure 1, collected from the frozen solution at 77 K shows an axial signal with a two-line hyperfine pattern arising from the I = 1/2 of 100% naturally abundant ^{89}Y, similar to those previously observed in yttrium reduction reactions.[1,25] The spectrum could be simulated to give $g_{\|}$ = 2.001 and $g_{\perp}$ = 1.981 with an average hyperfine coupling constant of A_{avg} = 62.8 G. After the room temperature measurement was completed, the sample had already decomposed to a pale orange/yellow solution. The observed 62.8 G hyperfine coupling constant fits in well with the data in Table 1 in that the value is high compared to other substituted cyclopentadienyl ligands, which is suggestive of increasing electron donation to the cyclopentadienide ring. Attempts to isolate the reactive Y(II) complex were not successful.

Neodymium. Nd was chosen for further studies for two reasons. Following the isolation and structural characterization of the Pu(II) complex, [K(crypt)][Cp''_3Pu] [crypt = 2.2.2-cryptand, Cp″ = $C_5H_3(SiMe_3)_2$],[16] it became of interest to expand the isolation of the +2 oxidation state to another transuranic metal, americium, with other cyclopentadienyl ligand sets. Neodymium was chosen as an appropriate model for this investigation, since the predicted nine-coordinate Nd(II) ionic radius of 1.35 Å is similar to the 1.31 Å of the predicted nine-coordinate Am(II) ionic radius.[42] Nd was also of interest, since Nd(II) is a configurational crossover ion and could conceivably form a traditional $4f^{n+1}$ complex that would have better stability than the "$(Cp^{tet}_3Y)^{1-}$" complex above. Nd is also considerably larger than yttrium, and the steric match of ligand set with metal size could be more favorable.

The reaction of Cp^{tet}_3Nd (Cp^{tet} = C_5Me_4H), **1-Nd**, with KC_8 in the presence of crypt in THF under argon at −35 °C produced a dark green solution. The product was crystallized from the THF solution by layer diffusion with Et_2O at −35 °C,

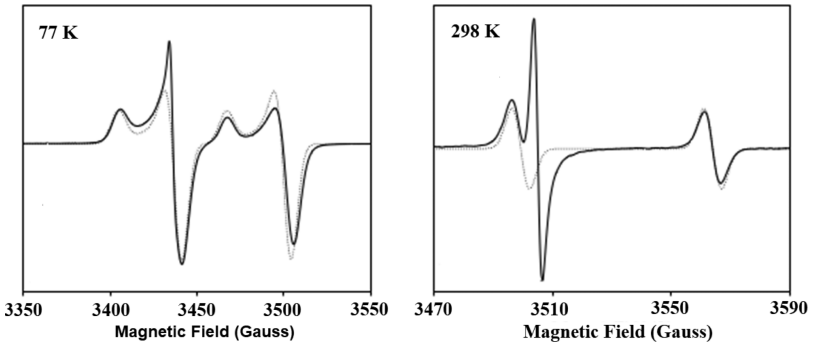

Figure 1. X-band EPR spectra of the reduction product of Cp^{tet}_3Y, **2-Y**, collected at 77 K (left; mode: perpendicular; $g_{\|}$ = 2.001, $g_{\perp}$ = 1.981; A_{avg} = 62.8 G; ν = 9.624 GHz; P = 2.026; modulation amplitude = 0.0407 mT) and 298 K (right; mode: perpendicular; g_{iso} = 1.986 ; A_{iso} = 64.8 G; ν = 9.817 GHz; P = 2.021; modulation amplitude = 2.853 mT). The simulated spectra (dotted lines) were generated with the exclusion of the extra feature in the right spectrum attributed to an electride species.[41]

DOI: 10.1021/acs.organomet.8b00557
Organometallics 2018, 37, 3863−3873

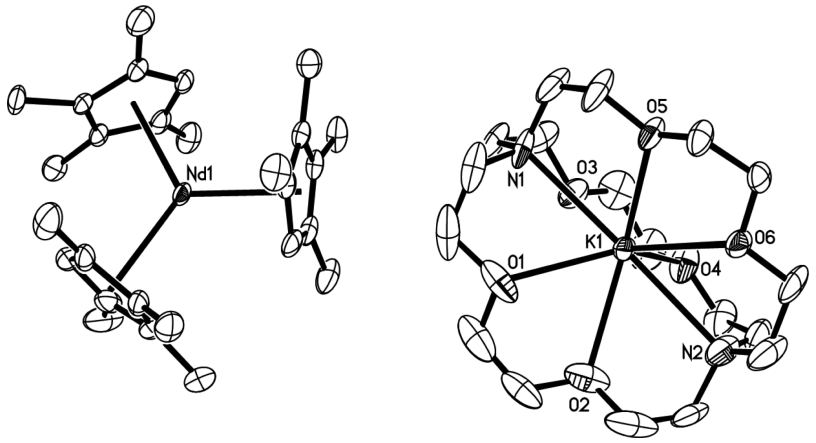

Figure 2. Thermal ellipsoid plot of [K(crypt)][Cp^{tet}_3Nd], **2-Nd**, drawn at 50% probability level. Hydrogen atoms are omitted for clarity.

and it was identified by X-ray crystallography as the Nd(II) complex, [K(crypt)][Cp^{tet}_3Nd], **2-Nd**, Figure 2, eq 1.

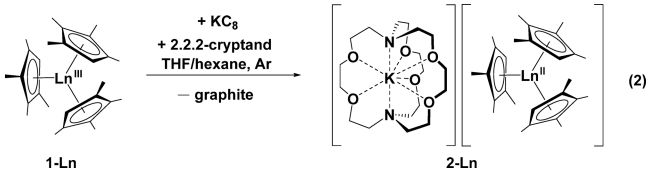

The Nd–ring centroid distances of **2-Nd** range between 2.555 and 2.568 Å with an average of 2.563 Å. This is 0.045 Å longer than the 2.518 Å Nd–ring centroid distance of the Nd(III) precursor, **1-Nd**.[43] This small change from Ln(III) to Ln(II) is consistent with that observed in going from $4f^n$ to $4f^n5d^1$ electron configurations with the new ions in the [K(crypt)][Cp'_3Ln], **3-Ln**, series.[10] In contrast, $4f^n$ to $4f^{n+1}$ reductions with the traditional ions, Eu(II), Yb(II), Sm(II), and Tm(II), give bond distance changes of 0.1–0.2 Å.[1−6] The small change in distances between the Nd(III) and Nd(II) complexes suggests that the added electron occupies the d_{z^2} orbital.

La, Ce, Pr, Sm, Gd, Tb, and Dy. Following the successful isolation of **2-Nd**, the syntheses of [K(crypt)][Cp^{tet}_3Ln] complexes were pursued across the lanthanide series. In the case of Ln = La, Ce, Pr, Sm, Gd, Tb, and Dy, reduction can be achieved with potassium graphite in the presence of crypt at −35 °C. The resulting dark solutions are stable enough to provide crystals of [K(crypt)][Cp^{tet}_3Ln], **2-Ln**. These crystals were grown over several days by transferring a freshly prepared THF solution of the sample to the bottom of a cooled vial of Et_2O for slow layer diffusion. Crystallographic data were collected on all of these samples which provided a new series of Ln(II) ions in a single coordination environment for comparison with the **3-Ln** series.[9,11,12] The Nd structure in Figure 2 is representative of these complexes, and spectroscopic data are presented later. It should be noted that mixed ether solvent occupancy was found in the lattice for Pr, Nd, Sm, Gd, Tb, and Dy, but no solvents were found in the crystal lattice of the complexes of the largest metals, La and Ce (see the Supporting Information for details).

Ho and Er. Attempts to make the Ho and Er analogues also gave dark solutions, but they did not persist for more than a few hours even at −35 °C and were not pursued further. This instability was consistent with that of the similarly sized yttrium complex.

EPR Spectra. The EPR spectra of [K(crypt)][Cp^{tet}_3La], **2-La**, and [K(crypt)][Cp^{tet}_3Gd], **2-Gd**, are shown in Figure 3. The eight-line hyperfine pattern of **2-La** is as expected for La(II), since the 99.9% naturally abundant ^{139}La has an $I = 7/2$ nuclear spin. The data are consistent with $g = 1.98$ and $A = 291$. The average hyperfine coupling constant for **2-La** is larger than the values found for **3-La**,[10] 154 G, and [K(crypt)]-[Cp''_3La],[7] 133.5 G, as well as the reduction product of Cp^{Me}_3La,[44] 195 G, as expected for the more electron donating Cp^{tet} ligand. The spectrum of **2-Gd** is similar to that of the crystallographically characterized **3-Gd**,[9] as well as the

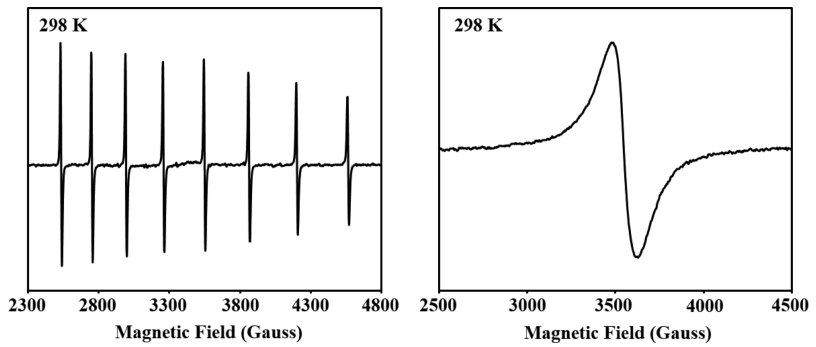

Figure 3. Room temperature EPR spectra of [K(crypt)][Cp^{tet}_3La] (left; mode: perpendicular; $g_{iso} = 1.97$; $A_{iso} = 291$ G; $\nu = 9.8175$ GHz; $P = 2.021$; modulation amplitude = 1 mT) and [K(crypt)][Cp^{tet}_3Gd] (right; mode: perpendicular; $g_{iso} = 1.9786$; $\nu = 9.8182$ GHz; $P = 2.026$; modulation amplitude = 1.464 mT).

DOI: 10.1021/acs.organomet.8b00557
Organometallics 2018, 37, 3863–3873

reduction products of Cp''_3Gd, Cp''_2GdCp, and Cp''_2GdCp^{Me}.[25]

Structural Analysis. Metrical parameters on the [K(crypt)][Cp^{tet}_3Ln], **2-Ln**, series are presented in Table 2,

Table 2. Comparison of Ln−(Cyclopentadienyl Ring Centroid) Distances (Ln−Cnt) for [K(crypt)][Cp^X_3Ln] with Cp^X = Cp^{tet}, Cp′, and Cp″

	Ln−Cnt range (Å)	$Ln-Cnt_{Ave}$ (Å)	Δ[Ln(II) vs Ln(III)][a]
$(Cp^{tet}_3La)^{1-}$	2.626−2.642	2.633	0.058[45]
$(Cp''_3La)^{1-}$	2.606−2.642	2.620	0.018[7,46]
$(Cp'_3La)^{1-}$	2.581−2.595	2.586	0.026[10,38]
$(Cp^{tet}_3Ce)^{1-}$	2.594−2.612	2.603	0.051[47]
$(Cp''_3Ce)^{1-}$	2.574−2.609	2.587	0.022[8,48]
$(Cp'_3Ce)^{1-}$	2.553−2.567	2.558	0.029[10,48]
$(Cp^{tet}_3Pr)^{1-}$	2.572−2.583	2.578	0.046[47]
$(Cp''_3Pr)^{1-}$	2.552−2.588	2.566	*b*
$(Cp'_3Pr)^{1-}$	2.530−2.544	2.535	0.026[9,49]
$(Cp^{tet}_3Nd)^{1-}$	2.555−2.568	2.563	0.045[43]
$(Cp''_3Nd)^{1-}$	2.530−2.559	2.544	0.019[8,46]
$(Cp'_3Nd)^{1-}$	2.514−2.528	2.519	0.031[10,49]
$(Cp^{tet}_3Sm)^{1-}$	2.623−2.640	2.630	0.147[45]
$(Cp'_3Sm)^{1-}$	2.603−2.615	2.608	0.148[10]
$(Cp^{tet}_3Gd)^{1-}$	2.511−2.519	2.516	0.047
$(Cp'_3Gd)^{1-}$	2.463−2.475	2.468	0.031[9]
$(Cp^{tet}_3Tb)^{1-}$	2.498−2.505	2.502	0.054[45]
$(Cp'_3Tb)^{1-}$	2.448−2.461	2.454	0.032[9]
$(Cp^{tet}_3Dy)^{1-}$	2.543−2.543	2.543	0.099
$(Cp'_3Dy)^{1-}$	2.434−2.450	2.443	0.036[10]

[a]Δ[Ln(II) vs Ln(III)] = the difference in Ln−Cnt distances of $[Cp^x_3Ln^{II}]^{1-}$ vs $Cp^x_3Ln^{III}$. The references are to the structures of the $Cp^x_3Ln^{III}$ complexes. [b]The structure of Cp''_3Pr has not been reported for comparison.[8]

along with data on the analogous [K(crypt)][Cp'_3Ln], **3-Ln**,[9−12] and [K(crypt)][Cp''_3Ln][7,8] complexes when available. The Ln−(C_5Me_4H ring centroid) distances (Ln−Cnt) for six of the eight **2-Ln** complexes with Ln = La, Ce, Pr, Nd, Gd, and Tb are consistent with Ln ionic radii, decreasing with increasing atomic number, following the lanthanide contraction. For each of these six metals, the Ln−Cnt distance also decreases in the order: $Cp^{tet} \gg Cp'' > Cp'$. This suggests that the $(Cp^{tet}_3)^{3-}$ environment occupies more space than $(Cp''_3)^{3-}$, which is surprising given that $(Cp'')^{1-}$ was investigated as a ligand for being sterically similar to $(C_5Me_5)^{1-}$.[50]

The differences in Ln−Cnt distances between the Ln(III) $(C_5R_5)_3Ln$ precursor and the reduced Ln(II) product for La, Ce, Pr, Nd, Gd, and Tb are 0.045−0.058 Å for the Cp^{tet} series versus 0.018−0.022 Å for the Cp″ complexes and 0.026−0.031 Å for the Cp′ compounds. All of these differences are much smaller than the 0.1−0.2 Å differences found for $4f^{n+1}$ Ln(II) versus $4f^n$ Ln(III) complexes of the traditional Ln(II) ions of Eu, Yb, Sm, and Tm. This is structural evidence consistent with $4f^n5d^1$ configurations for these six metals based on previous structural, spectroscopic, and DFT analysis of the **3-Ln** complexes.[9−12]

Sm and Dy. The metrical parameters of the samarium and dysprosium complexes, **2-Sm** and **2-Dy**, differ from those of the six metals above. The difference in Ln−Cnt distances between the Ln(II) complexes and their Ln(III) precursors are 0.147 and 0.099 Å for **2-Sm** and **2-Dy**, respectively. This is substantially larger than the 0.045−0.058 Å differences for the six other metals in the series. These larger distances suggest that **2-Sm** and **2-Dy** contain $4f^6$ and $4f^{10}$ ions, respectively, and not $4f^n5d^1$ species. These metrical parameters and $4f^{n+1}$ electronic configuration assignments are consistent with the UV−vis spectra presented below. This is also reasonable, since Sm is known as a traditional Ln(II) ion and Dy is known as a configurational crossover ion.[10] The difference in these two structures is shown graphically in Figure 4, which plots Ln−

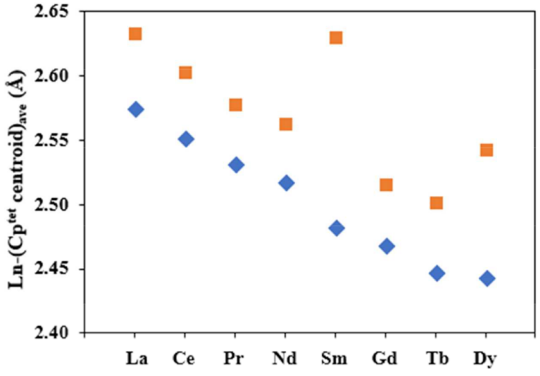

Figure 4. Plot of average Ln−(Cp^{tet} centroid) distances in Cp^{tet}_3Ln, **1-Ln** (blue diamonds), and in **2-Ln** (orange squares).

Cnt distances as a function of atomic number. In addition, the Evans method[51−53] magnetic moment of **2-Dy** is 10.8 μ_B. This is close to the 10.6 μ_B theoretical value for a $4f^{10}$ complex and is smaller than the 11.3−11.7 μ_B values observed for $4f^95d^1$ complexes.[24]

UV−vis Spectroscopy. The UV−vis spectra of **2-Ln** are shown in Figure 5, and the absorbance maxima and extinction coefficients are compared with those of **3-Ln** in Table 3. The spectra of **2-Ln** for Ln = La, Ce, Pr, Nd, Gd, and Tb show the strongest absorptions in the near-infrared region with λ_{max} values in the range 745−874 nm with a molar extinction coefficient, ε, of 1700−5600 M^{-1} cm^{-1}, Figure 5. In comparison, the previously reported spectra of **3-Ln** complexes of these metals have the largest absorptions from 420 to 635 nm in the visible region with ε = 4400−6500 M^{-1} cm^{-1}.[1,2,9−12]

In contrast to the UV−vis spectra of La, Ce, Pr, Nd, Gd, and Tb, the spectra of **2-Dy** and **2-Sm** have weaker absorptions. These are shown with a different scale in Figure 5 (right). Less intense absorptions were previously observed for the **3-Ln** complexes for the metals with $4f^{n+1}$ electron configurations, i.e., Eu, Yb, Sm, and Tm.[10] Hence, the λ_{max} = 466 nm with ε = 203 M^{-1} cm^{-1} for **2-Sm** is consistent with a $4f^6$ electron configuration for this complex. The weaker absorption for **2-Dy** with λ_{max} = 766 nm and ε = 200 M^{-1} cm^{-1} is also consistent with a $4f^{n+1}$ configuration, and this matches the structural data above which suggested that **2-Dy** had a $4f^{10}$ configuration.

Theoretical Analysis. The structures of the Cp^{tet}_3Ln precursors and the $(Cp^{tet}_3Ln)^{1-}$ anions in the **2-Ln** complexes were optimized with density functional theory (DFT) using the Tao−Perdew−Staroverov−Scuseria meta-generalized gradient approximation hybrid (TPSSh) density functional along with split valence basis sets[54] for the ligands and quasi-relativistic f-in-core effective core potentials (ECPs)[55] for **2-La**, **3-La**, **2-Ce**, **3-Ce**, **2-Sm**, **3-Sm**, **2-Gd**, and **3-Gd** (see the Supporting Information for further details); f-in-core electron

DOI: 10.1021/acs.organomet.8b00557
Organometallics 2018, 37, 3863−3873

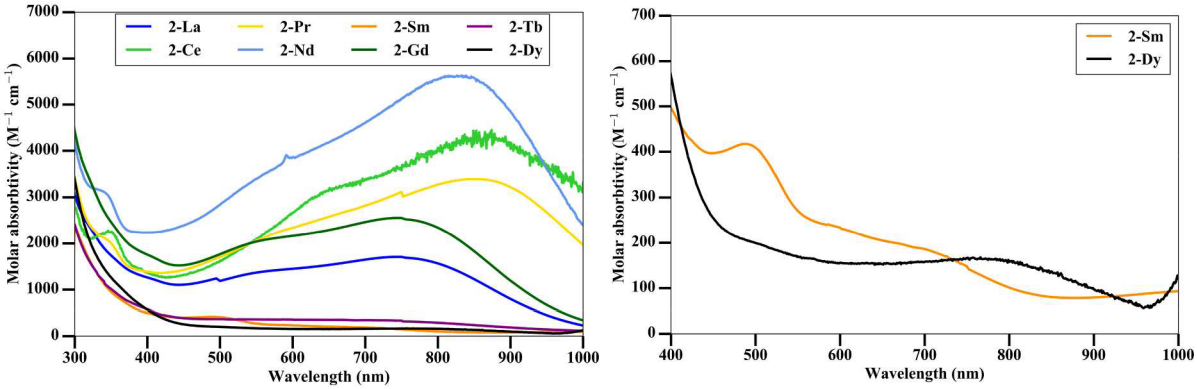

Figure 5. UV−vis spectra of **2-Ln** (Ln = La, Ce, Pr, Nd, Sm, Gd, Tb, Dy) collected at 5.0 mM concentration in THF at room temperature on the left and expanded scale spectra of **2-Dy** and **2-Sm** on the right.

Table 3. Comparison of UV−vis Absorption Maxima of [K(crypt)][Cp$^{tet}_3$Ln], 2-Ln, and [K(crypt)][Cp′$_3$Ln], 3-Ln

	λ_{max} (nm)	ε (M^{-1} cm^{-1})
2-La	745	1700
3-La[10]	554	6500
2-Ce	874	4100
3-Ce[10]	635	4700
2-Pr	854	4500
3-Pr[9]	518	4500
2-Nd	833	5600
3-Nd[10]	420	4700
2-Sm	466	200
3-Sm[10]	360	700
2-Gd	745	2500
3-Gd[9]	430	4400
2-Tb	784	650
3-Tb[9]	464	4800
2-Dy	766	200
3-Dy[10]	483	3400

configurations are denoted by brackets in the following discussion. This methodology was previously established for the **3-Ln** series[9] and further validated by f-out-of-core calculations[56] for **2-La**, **3-La**, **2-Ce**, **3-Ce**, **3-Pr**, **2-Sm**, **3-Sm**, **2-Gd**, and **3-Gd** (see the Supporting Information for further details).

For the La, Ce, Pr, Nd, Gd, and Tb anions in **2-Ln**, the calculated average Ln−(Cp ring centroid) distances are within 0.001−0.02 Å of the experimental values. Moreover, for these six metals, the computed change in Ln−Cnt distances between the Ln(III) precursor Cp$^{tet}_3$Ln and the reduced Ln(II) product, **2-Ln**, matches the X-ray data within 0.02 Å when [4f^n]5d^1 configurations for the anions are assumed with the f-in-core effective core potentials (Table S24, Supporting Information). The highest occupied molecular orbital of **2-La** is shown in Figure 6. The 5d$_{z^2}$ nature of this HOMO matches those found for **3-Ln**.

Since Nd(II) is a configurational crossover ion that has been observed to access both 4f^4 and 4f^{3}5d^1 electron configurations, calculations on (Cp$^{tet}_3$Nd)$^{1-}$ with a [4f^4] electron configuration were also carried out. With this traditional electronic configuration, a 2.727 Å Nd−Cnt distance is predicted which is much longer than the experimentally observed value of 2.563 Å. Also, no appreciable absorptions are predicted in the visible spectrum, in contrast to the strong experimental absorbance.

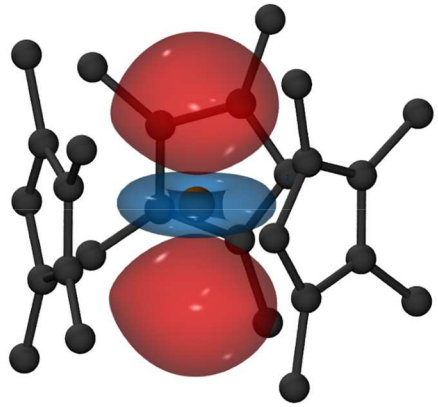

Figure 6. Highest singly occupied molecular orbital of **2-La** (contour value 0.04 au), obtained using DFT with the TPSSh functional and the f-in-core SCecp-mwb-d ECP (see the Supporting Information for details).

The f-out-of-core calculations converged to a predominantly 4f^4 state but with a Nd−centroid distance of 2.621 Å. Calculations with a [4f^3]5d^1 configuration gave a value of 2.580 Å, closer to the metrical parameters from the X-ray crystal structure, and excitation spectra in qualitative agreement with experiment (see below). These results provide support for the assignment of **2-Nd** as a 4f^{3}5d^1 ion with a low-lying excited 4f^4 configuration.

In contrast to the results above, calculations on the traditional Sm(II) ion with a [4f^6] electron configuration in (Cp$^{tet}_3$Sm)$^{1-}$ led to a 2.696 Å, Sm−Cnt distance which is longer than the 2.630 Å observed distance. However, f-out-of-core calculations predicted a 4f^6 configuration with a 2.610 Å Sm−centroid distance in close agreement with experiment. For the configurational crossover ion Dy(II), the calculated bond distance for neither the [4f^{10}] configuration, 2.650 Å, nor the [4f^9]5d^1 configuration, 2.505 Å, matched the 2.543 Å observed value. However, the calculated differences in Ln−ring centroid distances of the Ln(III) Cp$^{tet}_3$Ln and the Ln(II) (Cp$^{tet}_3$Ln)$^{1-}$ for Sm and Dy, 0.200 and 0.199 Å, respectively, were much larger than those of the 4f^{n}5d^1 ions described above. The experimentally observed Ln(II) vs Ln(III) differences for Sm and Dy, 0.147 and 0.099 Å, are not as large as the calculated differences, but the data support the presence of 4f^{n+1} configurations for the ions in (Cp$^{tet}_3$Sm)$^{1-}$ and (Cp$^{tet}_3$Dy)$^{1-}$, which is consistent with the UV−vis data. Time-dependent density functional theory (TDDFT) simulations are consistent

DOI: 10.1021/acs.organomet.8b00557
Organometallics 2018, 37, 3863−3873

with this view and qualitatively reproduce the much stronger visible absorption of the La, Ce, Pr, Nd, Gd, and Tb compounds compared to the Sm and Dy compounds; see Figure 7.

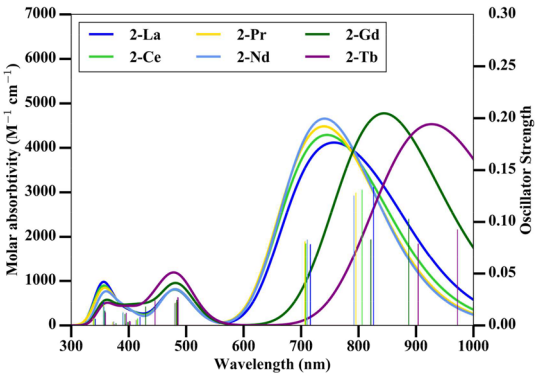

Figure 7. Predicted spectra from TDDFT using the TPSSh functional and the f-in-core SCecp-mwb-d ECP (see the Supporting Information for details).

Analysis of time-dependent density functional theory (TDDFT) simulations for the $(Cp^{tet}Ln)^{1-}$ (Ln = La, Ce, Pr, Nd, Gd, and Tb) compounds reveals that, in addition to the MLCT absorptions found previously in the **3-Ln** series, there are strongly dipole-allowed Ln 5d → 6p and 5d → π^* transitions (Table S26, Supporting Information) at lower energy. The three distinct bands in the computed visible spectra can be associated with transitions to 6p Rydberg orbitals of slightly different energies. The higher oscillator strengths for the 5d → 6p transitions in the **2-Ln** series can be rationalized by the larger metal−ligand distances in these compounds, which stabilize metal 6p Rydberg orbitals relative to the **3-Ln** compounds. MLCT transitions are still present in **2-Ln** (Ln = La, Ce, Pr, Nd, Gd, and Tb), but they are much weaker than these 5d → 6p transitions. It should also be noted that 5d → 6p absorptions are also present in **3-Ln**, but they are weaker in those complexes.

Geometric effects may also be operative in the difference in intensities of the transitions in **2-Ln** vs **3-Ln**. The C_{3h} **2-Ln** complexes are more symmetrical when compared to the **3-Ln** species. In the **3-Ln** series, two of the Me_3Si substituents are above the plane defined by the metal and the three Cp′ ring centroids and one Me_3Si group is below. In the **2-Ln** series, the arrangement of substituents has a different symmetry: the one unique ring carbon atom is the C−H unit rather than the unique ring substituted C−$SiMe_3$ moiety in **3-Ln**. In **2-Ln**, these unique C−H positions are more similar in the three rings and are in or near the plane of the three ring centroids (see Supporting Information Table S2). As a result, there are six methyl groups above the plane of the three Cp^{tet} ring centroids and six below. These differences in molecular geometry could change the overlap of the occupied and virtual molecular orbitals, which results in the difference in oscillator strengths for the two types of transitions and the difference in extinction coefficients in the spectra.

Thermal Stability. The stability of the **2-Ln** complexes of the larger metals, Ln = La, Ce, Pr, Nd, Sm, and Gd, is greater than that of Ln = Tb, Dy, Ho, Er, and Y. For the larger metals, the dark blue/black solutions obtained by reduction with KC_8 in THF, followed by Et_2O layer diffusion at room temperature, are stable for at least 48 h. However, for Dy, the reduction must be done at −35 °C in order to isolate a dark-colored product. For Ho, Er, and Y, reductions, even at −35 °C, yield unstable black solutions that do not persist longer than 12 h at −35 °C. Only the dark-colored solutions of **3-La**, **3-Ce**, and **3-Nd** persist as long as the larger members of the **2-Ln** series with Ln = La−Gd. Hence, it appears that the **2-Ln** complexes of the larger lanthanides are more stable than the **3-Ln** analogues.

The thermal decomposition of **2-Tb** was examined in a manner analogous to previous studies on **3-Ln** and [K(crypt)][Cp''_3Ln][8,9] by monitoring the decrease in the maximum absorbance in the UV−vis spectrum, in this case at λ_{max} = 784 nm. The data on **2-Tb** were best modeled with second order kinetics (see the Supporting Information), which is consistent with previous Ln(II) decomposition studies.[8,9] The observed second order rate constant of 5.4(7) × 10^{-2} M^{-1} cm^{-1} is an order of magnitude larger than the second order rate constant, 4.25(5) × 10^{-3} M^{-1} cm^{-1}, observed for **3-Tb**.[9] Hence, for this smaller metal, the **2-Tb** complex is less stable than the **3-Tb**.

DISCUSSION

Although Cp^{tet} was originally considered to be an unlikely ligand to stabilize $4f^n5d^1$ Ln(II) ions because it is so electron donating, it has provided crystallographically characterizable tris(cyclopentadienyl) Ln(II) complexes for La, Ce, Pr, Nd, Gd, and Tb, as well as the traditional Sm(II) and configurational crossover Dy(II). The EPR data on [K(crypt)][Cp^{tet}_3La], **2-La**, and the product of reducing Cp^{tet}_3Y show larger hyperfine coupling values consistent with more electron density on the metal. Previously, reducing the electron density on the metal was thought to be critical in isolating Ln(II) complexes. Given the isolation of these **2-Ln** complexes, it is clear that cyclopentadienyl ligands with alkyl substituents are not too electron donating to form Ln(II) complexes of this type. The isolation of the **2-Ln** complexes as well as a series of $[Ln(NR_2)_3]^{1-}$ complexes[40] show that using the hyperfine coupling constant value for yttrium as a gauge for predicting the stability of Ln(II) complexes is not appropriate! It remains to be determined if this is a special aspect of yttrium and its 4d orbitals.

There are two major differences between [K(crypt)][Cp^{tet}_3Ln], **2-Ln**, and the previously reported [K(crypt)][Cp'_3Ln], **3-Ln**, series. One notable difference for the six $4f^n5d^1$ ions of La, Ce, Pr, Nd, Gd, and Tb is that the Ln−Cnt distances for the Ln(II) Cp^{tet} complexes, **2-Ln**, are 0.043−0.048 Å longer than those of the analogous Ln(II) Cp′ complexes, **3-Ln**. Hence, although the Cp^{tet} ligands may be more electron donating, they are further away from the metal. This may mitigate their greater electron donating ability and allow the isolation of Ln(II) complexes for these metals. Of course, the Cp^{tet} ligands also provide more steric protection for the metal with their four substituents compared to the monosubstituted Cp′. The importance of steric saturation to the stability of Ln(III) complexes is well established.

It is interesting to note that the difference in metal−Cnt distances between **2-Ln** and **3-Ln** for the traditional Sm(II) complexes is only 0.022, whereas the difference for the configurational crossover Dy(II) complex is 0.10 Å. Hence, these $4f^{n+1}$ systems do not show regularity in the difference in metal−ring centroid distances between Cp^{tet} and Cp′ ligand systems.

DOI: 10.1021/acs.organomet.8b00557
Organometallics 2018, 37, 3863−3873

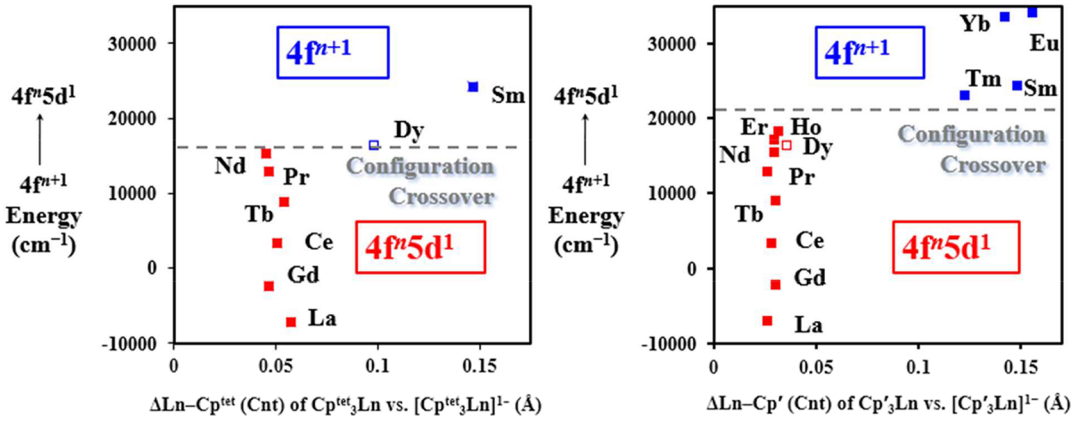

Figure 8. Plot of the $4f^{n+1}$ to $4f^n5d^1$ promotion energy compared to the change in distance upon reduction of Cp^x_3Ln to $(Cp^x_3Ln)^{1-}$ for $Cp^x = Cp^{tet}$ (left) and $Cp^x = Cp'$ (right).

Another notable difference between **2-Ln** and **3-Ln** involves the UV−vis spectra. The absorptions with the largest λ_{max} values are at lower energies compared to the most intense absorptions of **3-Ln** for Ln = La, Ce, Pr, Nd, Gd, and Tb. TDDFT studies indicate that the maximum absorbances for the two series do not arise from analogous transitions. For **2-Ln**, the most intense absorptions arise from Ln 5d → 6p transitions; for **3-Ln**, the largest absorptions are attributed to MLCT. While both transitions are present in both complexes, the MLCT transitions are more intense for **3-Ln** and the metal−metal transitions are more intense for **2-Ln**. It is likely that the longer metal−ligand distances in **2-Ln** weaken the MLCT and enhance the 5d → 6p transitions. The difference in intensities of the two series could also occur due to the difference in the geometry of the complexes. In addition to the changes in metal−ligand distance, the higher molecular symmetry of the **2-Ln** complexes could be the cause of greater metal p-character in lower energy unoccupied MOs, which would have a stronger oscillator strength due to a large 5d → 6p transition dipole moment.

In the $[K(crypt)][Cp^{tet}_3Ln]$, **2-Ln**, series, both the crystallographic data and the UV−vis data suggest that $4f^n5d^1$ ions are present for La Ce, Pr, Nd, Gd, and Tb and $4f^{n+1}$ ions for Sm and Dy. This is supported by the DFT calculations (see the Supporting Information). This dichotomy differs from that with the $[K(crypt)][Cp'_3Ln]$, **3-Ln**, series where the Dy complex was assigned a $4f^n5d^1$ electron configuration. This is consistent with the realization that the ligand field can affect the configurations involving the 5d orbitals and demonstrates that changing the substitution on the cyclopentadienyl rings can change the border between $4f^n5d^1$ and $4f^{n+1}$ configurations. This is shown graphically in Figure 8 where the differences in Ln−Cnt distances for Ln(II) and Ln(III) analogues are plotted versus the $4f^{n+1}$ to $4f^n5d^1$ promotion energy determined from gas phase atomic spectra of +2 ions.[57] The dotted line border between traditional and nontraditional electron configurations has changed for Cp^{tet} compared to Cp′. It is interesting to note that attempts to make **2-Ho** and **2-Er** in this study led to solutions too reactive to isolate. According to Figure 5, which is admittedly a simplistic analysis of the system, **2-Ho** and **2-Er** could be $4f^{n+1}$ ions in the $(Cp^{tet}_3)^{3-}$ coordination environment. Calculations of $4f^n$ Ln(III) to $4f^{n+1}$ Ln(II) reduction potentials for Ho and Er are −2.9 and −3.1 V, respectively; i.e., they could be more reactive than Ho(II) and Er(II) ions in the **3-Ln** complexes which have reduction potentials less negative than −2.9 V.

CONCLUSION

The isolation of $(Cp^{tet}_3Ln)^{1-}$ complexes for Ln = La, Ce, Pr, Nd, Gd, and Tb indicates that the prior assumption that electron-rich cyclopentadienyl ligands cannot be used to isolate $4f^n5d^1$ Ln(II) complexes is incorrect. More generally, this suggests that the new mixed configuration Ln(II) ions are likely to be accessible with a variety of ligand systems. This will allow a broader investigation of both their physical properties and their reactivity. In addition, the results show the importance of the ligand in determining which configuration, $4f^{n+1}$ or $4f^n5d^1$, is adopted by Ln(II) ions in tris(cyclopentadienyl) coordination environments. The crossover point between the two configurations is variable depending on the ligands. Thus, judicious choice of the ligand environment may profoundly affect the chemical, optical, and magnetic properties of divalent lanthanides which can be significantly different for $4f^{n+1}$ vs $4f^n5d^1$ configurations.

EXPERIMENTAL DETAILS

All manipulations and syntheses described below were conducted with rigorous exclusion of air and water using standard Schlenk line and glovebox techniques under an argon atmosphere. Solvents were sparged with UHP argon (Airgas) and dried by passage through columns containing Q-5 and molecular sieves prior to use. THF-d_8 (Cambridge Isotope Laboratories) was dried over NaK alloy, degassed by three freeze−pump−thaw cycles, and vacuum transferred before use. KC_8[58] was prepared as previously described. KCp^{tet} (Cp^{tet} = C_5Me_4H) and Cp^{tet}_3Ln (Ln = Y,[59] La,[45] Ce,[47] Pr,[47] Nd,[43] Sm,[45] Tb[45]), **1-Ln**, were synthesized using modified literature procedures. 2.2.2-Cryptand (4,7,13,16,21,24-hexaoxa-1,10-diazabicyclo[8,8,8]-hexacosane, VWR) was held under a vacuum (1 mTorr) for 12 h prior to use. The Evans method magnetic susceptibility[51−53] was obtained on a CRYO500 MHz spectrometer at 298 K unless otherwise stated and referenced internally to residual protio-solvent resonances. UV−vis measurements were conducted at 298 K in THF with a Jasco 670 UV−vis-NIR spectrophotometer. IR samples were prepared as KBr pellets on a Jasco FT/IR-4700 spectrometer. Elemental analyses were conducted on a PerkinElmer 2400 Series II CHNS elemental analyzer.

Synthesis of $(C_5Me_4H)_3Gd$, 1-Gd. After $GdCl_3$ (0.110 g, 0.418 mmol) was stirred in THF (10 mL) for 2 h, KCp^{tet} (0.201 g, 1.257 mmol) was added and the mixture was stirred for 12 h. The solvent was removed, toluene (10 mL) was added, and the mixture has heated to reflux in a sealed flask under a slight vacuum (~85 °C) for 12 h.

DOI: 10.1021/acs.organomet.8b00557
Organometallics 2018, 37, 3863−3873

The mixture was centrifuged, and the supernatant was filtered to give a pale-yellow solution. Removal of the solvent (in vacuo) followed by trituration with hexane produced a pale yellow solid, **1-Gd** (0.111 g, 51%). Orange single crystals suitable for X-ray diffraction were obtained from a concentrated solution of toluene. IR (cm^{-1}): 3113m, 2962vs, 2905vs, 2885vs, 2722s, 2499w, 2046w, 1645w, 1580s, 1544s, 1484s, 1436vs, 1381vs, 1371vs, 1329s, 1173s, 1133m, 1107m, 1018s, 971s, 776vs, 699m, 610s. Anal. Calcd for $C_{27}H_{39}Gd$: C, 62.26; H, 7.55. Found: C, 59.87; H, 7.36. The results give a formula of $C_{27}H_{39.6}$. Obtaining satisfactory analysis on the new members of the known **1-Ln** series[43,45,47,60,61] as well as the **2-Ln** series has been unexpectedly challenging, although problems with elemental analyses of organolanthanides are well documented.[7,62−64] Multiple attempts have been made to get good data, but poor carbon combustion has been a problem.

Synthesis of $(C_5Me_4H)_3Dy$, 1-Dy. Similarly to **1-Gd**, KCp^{tet} (0.190 g, 1.185 mmol) was added stepwise to a solution of $DyCl_3$ (0.100 g, 0.372 mmol) in THF (10 mL). After reflux and collection of the resulting supernatant, a pale orange solid was obtained, **1-Dy** (0.1012 g, 95%). Orange single crystals suitable for X-ray diffraction were obtained from a concentrated solution of toluene. IR (cm^{-1}): 3117w, 2965s, 2901vs, 2856vs, 2723m, 1653m, 1436s, 1382s, 1327m, 1173m, 1141m, 1019s, 971s, 781vs, 668m, 608m. Anal. Calcd for $C_{27}H_{39}Dy$: C, 61.64; H, 7.47. Found: C, 57.54; H, 7.23. The low values suggest incomplete sample combustion. The results give a formula of $C_{27}H_{40.4}$.

Synthesis of [K(crypt)][$(C_5Me_4H)_3La$], 2-La. **1-La** (0.028 g, 0.056 mmol) and crypt (0.021 g, 0.057 mmol) were dissolved in THF (2 mL). The solution was cooled to −35 °C prior to addition of KC_8 (0.012 g, 0.085 mmol). The solution was immediately filtered, layered using chilled hexane, and left at −35 °C. A dark blue crystalline solid, identified as [K(crypt)][$(C_5Me_4H)_3La$], **2-La**, by X-ray diffraction, was obtained after 3 days (0.046 g, 89%). Single dark blue crystals of **2-La** suitable for X-ray diffraction were obtained by diffusion of the concentrated THF solution with Et_2O at −35 °C. IR (cm^{-1}): 3070w, 2962m, 2882s, 2820s, 2704w, 1477m, 1445m, 1353s, 1321w, 1293m, 1258m, 1239w, 1173w, 1133s, 1108vs, 1097s, 1017w, 951s, 933m, 833w, 750m, 733w. UV−visible (THF) λ_{max} nm (ε, M^{-1} cm^{-1}): 745 (1700). Anal. Calcd for $C_{45}H_{75}KN_2O_6La$: C, 58.87; H, 8.23; N, 3.05. Found: C, 58.81; H, 8.17; N, 3.36. The results give a formula of $C_{45}H_{74.5}N_{2.2}$.

[K(crypt)][$(C_5Me_4H)_3Ce$], 2-Ce. In a procedure analogous to the preparation of **2-La**, **1-Ce** (0.055 g, 0.11 mmol) and crypt (0.045 g, 0.12 mmol) were dissolved in THF (2 mL) and reacted with KC_8 (0.022 g, 0.16 mmol) to form a dark blue crystalline solid identified as [K(crypt)][$(C_5Me_4H)_3Ce$], **2-Ce** (0.112 g, 61%). Single dark blue crystals of **2-Ce** suitable for X-ray diffraction were obtained by layer diffusion of the concentrated THF solution with Et_2O at −35 °C. IR (cm^{-1}): 3074w, 2961m 2883s, 2820s, 2704w, 1477m, 1456m, 1444m, 1354m, 1295m, 1258m, 1134s, 1108vs, 1080s, 1018m, 951s, 933m, 833w, 749m, 734w. UV−visible (THF) λ_{max} nm (ε, M^{-1} cm^{-1}): 874 (4100). Anal. Calcd for $C_{45}H_{75}KN_2O_6Ce$: C, 58.79; H, 8.22; N, 3.05. Found: C, 58.04; H, 8.34; N, 3.66. The results give a formula of $C_{45}H_{77}N_{2.4}$.

[K(crypt)][$(C_5Me_4H)_3Pr$], 2-Pr. Synthesis of [K(crypt)]-[$(C_5Me_4H)_3Pr$], 2-Pr. Similar to the preparation of **2-Pr**, **1-Pr** (0.015 g, 0.0274 mmol) and crypt (0.010 g, 0.0274 mmol) were dissolved in THF (2 mL) and reacted with KC_8 (0.005 mg, 0.03 mmol) to form a black crystalline solid of [**K(crypt)**][$(C_5Me_4H)_3Pr$], **2-Pr** (0.017 g, 76%). Single crystals of **2-Pr** suitable for X-ray diffraction were obtained by layer diffusion of the concentrated THF solution with Et_2O at −35 °C. IR (cm^{-1}): 3077w, 2961m, 2882s, 2821s, 2702w, 1477m, 1445m, 1354m, 1296m, 1258m, 1134s, 1109vs, 1080s, 952s, 933m, 833w, 749m, 734w. UV−visible (THF) λ_{max} nm (ε, M^{-1} cm^{-1}): 854 (4500). Anal. Calcd for $C_{45}H_{75}KN_2O_6Pr$: C, 58.74; H, 8.22; N, 3.04. Found: C, 57.15; H, 7.88; N, 3.60. The results give a formula of $C_{45}H_{74}N_{2.4}$.

[K(crypt)][$(C_5Me_4H)_3Nd$], 2-Nd. Similar to the preparation of **2-La**, **1-Nd** (0.040 g, 0.079 mmol) and crypt (0.030 g, 0.079 mmol) were dissolved in THF (2 mL) and reacted with KC_8 (0.013 g, 0.095 mmol) to form a black crystalline solid of **2-Nd** (0.033 g, 45%). Single crystals of **2-Nd** suitable for X-ray diffraction were obtained by layer diffusion of the concentrated THF solution with Et_2O at −35 °C. IR (cm^{-1}): 3080w, 2962m, 2883s, 2822s, 2704w, 1477m, 1444m, 1354m, 1323w, 1296m, 1258m, 1238w, 1173w, 1134s, 1109vs, 1081s, 951s, 933m, 832w, 749m, 700w. UV−visible (THF) λ_{max} nm (ε, M^{-1} cm^{-1}): 833 (5600). Anal. Calcd for $C_{45}H_{75}KN_2O_6Nd$: C, 58.53; H, 8.19; N, 3.03. Found: C, 56.96; H, 7.96; N, 1.72. The low values suggest incomplete sample combustion. The results give a formula of $C_{45}H_{75}N_{1.2}$.

[K(crypt)][$(C_5Me_4H)_3Sm$], 2-Sm. In a procedure analogous to the preparation of **2-La**, **1-Sm** (0.029 g, 0.056 mmol) and crypt (0.021 g, 0.056 mmol) were dissolved in THF (2 mL) and reacted with KC_8 (0.010 g, 0.074 mmol) to form a dark brown crystalline solid identified as [K(crypt)][$(C_5Me_4H)_3Sm$], **2-Sm** (0.023 g, 43%). Single dark brown crystals of **2-Sm** suitable for X-ray diffraction were obtained by layer diffusion of the concentrated THF solution with Et_2O at −35 °C. IR (cm^{-1}): 3037w, 2911s, 2882vs, 2851s, 2817m, 2755w, 2717w, 1958w, 1477m, 1450m, 1444m, 1353s, 1264m, 1259m, 1237m, 1119s, 1106vs, 1028w, 949s, 932m, 877m, 818s, 754m, 657m. UV−visible (THF) λ_{max} nm (ε, M^{-1} cm^{-1}): 466 (200). Anal. Calcd for $C_{45}H_{75}KN_2O_6Sm$: C, 58.15; H, 8.13; N, 3.01. Found: C, 56.34; H, 8.01; N, 3.34. The results give a formula of $C_{45}H_{76}N_{2.3}$.

[K(crypt)][$(C_5Me_4H)_3Gd$], 2-Gd. In a procedure analogous to the preparation of **2-La**, **1-Gd** (0.007 g, 0.01 mmol) and crypt (0.005 g, 0.01 mmol) were dissolved in THF (2 mL) and reacted with KC_8 (0.003 g, 0.02 mmol) to form a dark blue crystalline solid identified as [K(crypt)][$(C_5Me_4H)_3Gd$], **2-Gd** (0.011 g, 93%). Single dark blue crystals of **2-Gd** suitable for X-ray diffraction were obtained by layer diffusion of the concentrated THF solution with Et_2O at −35 °C. IR (cm^{-1}): 3087w, 2961m, 2880s, 2820s, 2702w, 1477m, 1445m, 1353s, 1293m, 1258m, 1118s, 1108vs, 1100s, 952s, 933m, 833w, 750m, 734m. UV−visible (THF) λ_{max} nm (ε, M^{-1} cm^{-1}): 745 (2500). Anal. Calcd for $C_{45}H_{75}KN_2O_6Gd$: C, 57.72; H, 8.07; N, 2.99. Found: C, 56.40; H, 7.87; N, 2.92. The results give a formula of $C_{45}H_{74.8}N_2$.

[K(crypt)][$(C_5Me_4H)_3Tb$], 2-Tb. In a procedure analogous to the preparation of **2-La**, **1-Tb** (0.032 g, 0.06 mmol) and crypt (0.028 g, 0.08 mmol) were dissolved in THF (2 mL) and reacted with KC_8 (0.015 g, 0.11 mmol) to form a dark blue crystalline solid identified as [K(crypt)][$(C_5Me_4H)_3Tb$], **2-Tb** (0.047 g, 83%). Single dark blue crystals of **2-Tb** suitable for X-ray diffraction were obtained by layer diffusion of the concentrated THF solution with Et_2O at −35 °C. IR (cm^{-1}): 3089w, 2961sm, 2882s, 2818s, 2701m, 1478m, 1444m, 1351m, 1295m, 1257m, 1134s, 1108vs, 1080s, 1078m, 952s, 933m, 832w, 822w, 749m, 734m, 603w, 567w, 525w. UV−visible (THF) λ_{max} nm (ε, M^{-1} cm^{-1}): 784 (650). Anal. Calcd for $C_{45}H_{75}KN_2O_6Tb$: C, 57.61; H, 8.06; N, 2.99. Found: C, 51.76; H, 6.83; N, 3.01. The results give a formula of $C_{45}H_{70.8}N_{2.2}$.

[K(crypt)][$(C_5Me_4H)_3Dy$], 2-Dy. Similar to the preparation of **2-La**, **1-Dy** (0.025 g, 0.05 mmol) and crypt (0.020 g, 0.05 mmol) were dissolved in THF (2 mL) and reacted with KC_8 (0.011 g, 0.08 mmol) to form a dark brown crystalline solid identified as [K(crypt)]-[$(C_5Me_4H)_3$ Dy], **2-Dy** (0.032 g, 68%). Single dark brown crystals of **2-Dy** suitable for X-ray diffraction were obtained by layer diffusion of the concentrated THF solution with Et_2O at −35 °C. IR (cm^{-1}): 3093w, 2955m, 2882vs, 2725w, 1475m, 1442m, 1353s, 1296m, 1258m, 1173w, 1118m, 1105vs, 1078s, 951s, 930m, 828w, 752m. UV−visible (THF) λ_{max} nm (ε, M^{-1} cm^{-1}): 766 (200). Anal. Calcd for $C_{45}H_{75}KN_2O_6Dy$: C, 57.40; H, 8.03; N, 2.97. Found: C, 56.34; H, 7.48; N, 3.08. The results give a formula of $C_{45}H_{71.2}N_{2.1}$.

X-ray Crystallographic Data. Crystallographic information for complexes **1-Ln** (Ln = Dy, Gd) and **2-Ln** (Ln = La, Ce, Pr, Nd, Sm Gd, Tb, Dy) is summarized in Table 1 and in the Supporting Information.

DOI: 10.1021/acs.organomet.8b00557
Organometallics 2018, 37, 3863−3873

■ ASSOCIATED CONTENT

Supporting Information

The Supporting Information is available free of charge on the ACS Publications website at DOI: 10.1021/acs.organomet.8b00557.

Details of crystallographic data collection, structure solution, and refinement, DFT calculation metrical data on **1-Ln** (Gd, Dy), **2-Ln** (La, Ce, Pr, Nd, Sm, Gd, Tb, Dy), and **3-Ln** (La, Ce, Pr, Nd, Sm, Gd, Tb, Dy) (PDF)

Accession Codes

CCDC 1857412−1857421 contain the supplementary crystallographic data for this paper. These data can be obtained free of charge via www.ccdc.cam.ac.uk/data_request/cif, or by emailing data_request@ccdc.cam.ac.uk, or by contacting The Cambridge Crystallographic Data Centre, 12 Union Road, Cambridge CB2 1EZ, UK; fax: +44 1223 336033.

■ AUTHOR INFORMATION

Corresponding Authors

*E-mail: filipp.furche@uci.edu.
*E-mail: wevans@uci.edu.

ORCID

Tener F. Jenkins: 0000-0002-9469-7405
David H. Woen: 0000-0002-5764-1453
Luke N. Mohanam: 0000-0002-7862-5153
Joseph W. Ziller: 0000-0001-7404-950X
Filipp Furche: 0000-0001-8520-3971
William J. Evans: 0000-0002-0651-418X

Notes

The authors declare no competing financial interest.

■ ACKNOWLEDGMENTS

We thank the U.S. National Science Foundation for support of the experimental studies (CHE-1565776 to W.J.E.) and the theoretical studies (CHE-1800431 to F.F.). For crystallographic assistance, we thank Michael Wojnar and Austin J. Ryan. We also thank Professor A. S. Borovik and the Laser Spectroscopy Facility for spectroscopic assistance.

■ REFERENCES

(1) Evans, W. J. Tutorial on the Role of Cyclopentadienyl Ligands in the Discovery of Molecular Complexes of the Rare-Earth and Actinide Metals in New Oxidation States. *Organometallics* **2016**, *35*, 3088−3100.

(2) Woen, D. H.; Evans, W. J. Expanding the + 2 Oxidation State of the Rare-Earth Metals, Uranium, and Thorium in Molecular Complexes. In *Handbook on the Physics and Chemistry of Rare Earths*; Bünzli, J.-C. G., Pecharsky, V. K., Eds.; Elsevier: Amsterdam, The Netherlands, 2016; Vol. *50*, pp 337−394.

(3) Meyer, G. Reduced Halides of the Rare-Earth Elements. *Chem. Rev.* **1988**, *88*, 93−107.

(4) Meyer, G. *The Divalent State in Solid Rare-Earth Metal Halides*; John Wiley & Sons: Chichester, U.K., 2012.

(5) Bochkarev, M. N. Molecular compounds of "new" divalent lanthanides. *Coord. Chem. Rev.* **2004**, *248*, 835−851.

(6) Nief, F. Molecular chemistry of the rare-earth elements in uncommon low-valent states. In *Handbook on the Physics and Chemistry of Rare Earths*; Gschneidner, K. A., Jr.; Bünzli, J.-C. G.; Pecharsky, V. K., Eds.; Elsevier Science: Amsterdam, The Netherlands, 2010; Vol. *40*, pp 241−300.

(7) Hitchcock, P. B.; Lappert, M. F.; Maron, L.; Protchenko, A. V. Lanthanum does form stable molecular compounds in the + 2 oxidation state. *Angew. Chem., Int. Ed.* **2008**, *47*, 1488−91.

(8) Palumbo, C. T.; Darago, L. E.; Windorff, C. J.; Ziller, J. W.; Evans, W. J. Trimethylsilyl versus Bis(trimethylsilyl) Substitution in Tris(cyclopentadienyl) Complexes of La, Ce, and Pr: Comparison of Structure, Magnetic Properties, and Reactivity. *Organometallics* **2018**, *37*, 900−905.

(9) MacDonald, M. R.; Bates, J. E.; Ziller, J. W.; Furche, F.; Evans, W. J. Completing the series of + 2 ions for the lanthanide elements: synthesis of molecular complexes of Pr^{2+}, Gd^{2+}, Tb^{2+}, and Lu^{2+}. *J. Am. Chem. Soc.* **2013**, *135*, 9857−68.

(10) Fieser, M. E.; MacDonald, M. R.; Krull, B. T.; Bates, J. E.; Ziller, J. W.; Furche, F.; Evans, W. J. Structural, spectroscopic, and theoretical comparison of traditional vs recently discovered Ln^{2+} ions in the $[K(2.2.2\text{-cryptand})][(C_5H_4SiMe_3)_3Ln]$ complexes: the variable nature of Dy^{2+} and Nd^{2+}. *J. Am. Chem. Soc.* **2015**, *137*, 369−82.

(11) MacDonald, M. R.; Ziller, J. W.; Evans, W. J. Synthesis of a crystalline molecular complex of Y^{2+}, $[(18\text{-crown-6})K][(C_5H_4SiMe_3)_3Y]$. *J. Am. Chem. Soc.* **2011**, *133*, 15914−7.

(12) MacDonald, M. R.; Bates, J. E.; Fieser, M. E.; Ziller, J. W.; Furche, F.; Evans, W. J. Expanding Rare-Earth Oxidation State Chemistry to Molecular Complexes of Holmium(II) and Erbium(II). *J. Am. Chem. Soc.* **2012**, *134*, 8420−8423.

(13) Langeslay, R. R.; Fieser, M. E.; Ziller, J. W.; Furche, F.; Evans, W. J. Synthesis, structure, and reactivity of crystalline molecular complexes of the $\{[C_5H_3(SiMe_3)_2]_3Th\}^{1-}$ anion containing thorium in the formal + 2 oxidation state. *Chemical Science* **2015**, *6*, 517−521.

(14) MacDonald, M. R.; Fieser, M. E.; Bates, J. E.; Ziller, J. W.; Furche, F.; Evans, W. J. Identification of the + 2 Oxidation State for Uranium in a Crystalline Molecular Complex, $[K(2.2.2\text{-Cryptand})][(C_5H_4SiMe_3)_3U]$. *J. Am. Chem. Soc.* **2013**, *135*, 13310−13313.

(15) Windorff, C. J.; MacDonald, M. R.; Meihaus, K. R.; Ziller, J. W.; Long, J. R.; Evans, W. J. Expanding the Chemistry of Molecular U^{2+} Complexes: Synthesis, Characterization, and Reactivity of the $\{[C_5H_3(SiMe_3)_2]_3U\}^-$ Anion. *Chem. - Eur. J.* **2016**, *22*, 772−82.

(16) Windorff, C. J.; Chen, G. P.; Cross, J. N.; Evans, W. J.; Furche, F.; Gaunt, A. J.; Janicke, M. T.; Kozimor, S. A.; Scott, B. L. Identification of the Formal + 2 Oxidation State of Plutonium: Synthesis and Characterization of $\{Pu(II)[C_5H_3(SiMe_3)_2]_3\}^-$. *J. Am. Chem. Soc.* **2017**, *139*, 3970−3973.

(17) Su, J.; Windorff, C. J.; Batista, E. R.; Evans, W. J.; Gaunt, A. J.; Janicke, M. T.; Kozimor, S. A.; Scott, B. L.; Woen, D. H.; Yang, P. Identification of the Formal + 2 Oxidation State of Neptunium: Synthesis and Structural Characterization of $\{Np^{II}[C_5H_3(SiMe_3)_2]_3\}^{1-}$. *J. Am. Chem. Soc.* **2018**, *140*, 7425−7428.

(18) Gun'ko, Y. K.; Hitchcock, P. B.; Lappert, M. F. Activation of a C−O bond by reaction of a tris(cyclopentadienyl)lanthanide complex with an alkali metal in dimethoxyethane (DME); crystal structures of $[Nd\{\eta\text{-}C_5H_3(SiMe_3)_2\text{-}1,3\}_2(\mu\text{-}OMe)_2Li(DME)]$ and $[\{Ce(\eta\text{-}C_5H_3{}^tBu_2\text{-}1,3)_2(\mu\text{-}OMe)_2\}]$. *J. Organomet. Chem.* **1995**, *499*, 213−219.

(19) Cassani, M. C.; Duncalf, D. J.; Lappert, M. F. The First Example of a Crystalline Subvalent Organolanthanum Complex: $[K([18]crown\text{-}6)\text{-}(\eta^2\text{-}C_6H_6)_2][(LaCp^{tt2})_2(\mu\text{-}\eta^6\text{:}\eta^6\text{-}C_6H_6)]\bullet 2C_6H_6$ (Cp^{tt}= η^5-$C_5H_3But_2$-1,3). *J. Am. Chem. Soc.* **1998**, *120*, 12958−12959.

(20) Jaroschik, F.; Nief, F.; Le Goff, X. F.; Ricard, L. Isolation of stable organodysprosium(II) complexes by chemical reduction of dysprosium(III) precursors. *Organometallics* **2007**, *26*, 1123−1125.

(21) Jaroschik, F.; Momin, A.; Nief, F.; Le Goff, X.-F.; Deacon, G. B.; Junk, P. C. Dinitrogen Reduction and C−H Activation by the Divalent Organoneodymium Complex $[(C_5H_2{}^tBu_3)_2Nd(\mu\text{-}I)K([18]\text{-}crown\text{-}6)]$. *Angew. Chem.* **2009**, *121*, 1137−1141.

(22) La Pierre, H. S.; Scheurer, A.; Heinemann, F. W.; Hieringer, W.; Meyer, K. Synthesis and characterization of a uranium(II) monoarene complex supported by delta backbonding. *Angew. Chem., Int. Ed.* **2014**, *53*, 7158−62.

(23) Fieser, M. E.; Ferrier, M. G.; Su, J.; Batista, E.; Cary, S. K.; Engle, J. W.; Evans, W. J.; Lezama Pacheco, J. S.; Kozimor, S. A.;

DOI: 10.1021/acs.organomet.8b00557
Organometallics 2018, 37, 3863−3873

Olson, A. C.; Ryan, A. J.; Stein, B. W.; Wagner, G. L.; Woen, D. H.; Vitova, T.; Yang, P. Evaluating the electronic structure of formal LnII ions in $Ln^{II}(C_5H_4SiMe_3)_3^{1-}$ using XANES spectroscopy and DFT calculations. *Chemical Science* **2017**, *8*, 6076−6091.
(24) Meihaus, K. R.; Fieser, M. E.; Corbey, J. F.; Evans, W. J.; Long, J. R. Record High Single-Ion Magnetic Moments Through $4f^n5d^1$ Electron Configurations in the Divalent Lanthanide Complexes $[(C_5H_4SiMe_3)_3Ln]^-$. *J. Am. Chem. Soc.* **2015**, *137*, 9855−9860.
(25) Corbey, J. F.; Woen, D. H.; Palumbo, C. T.; Fieser, M. E.; Ziller, J. W.; Furche, F.; Evans, W. J. Ligand Effects in the Synthesis of Ln^{2+} Complexes by Reduction of Tris(cyclopentadienyl) Precursors Including C−H Bond Activation of an Indenyl Anion. *Organometallics* **2015**, *34*, 3909−3921.
(26) Huh, D. N.; Kotyk, C. M.; Gembicky, M.; Rheingold, A. L.; Ziller, J. W.; Evans, W. J. Synthesis of rare-earth-metal-in-cryptand dications, $[Ln(2.2.2\text{-cryptand})]_{2+}$, from Sm^{2+}, Eu^{2+}, and Yb^{2+} silyl metallocenes $(C_5H_4SiMe_3)_2Ln(THF)_2$. *Chem. Commun.* **2017**, *53*, 8664−8666.
(27) Lauher, J. W.; Hoffmann, R. Structure and chemistry of bis(cyclopentadienyl)-MLn complexes. *J. Am. Chem. Soc.* **1976**, *98*, 1729−1742.
(28) Bursten, B. E.; Rhodes, L. F.; Strittmatter, R. J. Bonding in Tris(y5-cyclopentadienyl) Actinide Complexes. 2. On the Ground Electronic Configurations of "Base-Free" Cp,An Complexes (An = Th, Pa, U, Np, Pu). *J. Am. Chem. Soc.* **1989**, *111*, 2756−2758.
(29) Bursten, B. E.; Rhodes, L. F.; Strittmatter, R. J. Bonding in Tris(y5-cyclopentadienyl) Actinide Complexes. 3. Interaction of 7-Neutral, 7-Acidic, and 7-Basic Ligands with (T5-C5H5)3U. *J. Am. Chem. Soc.* **1989**, *111*, 2758−2766.
(30) Strittmatter, R. J.; Bursten, B. E. Bonding in Tris(η^5-Cyclopentadienyl) Actinide Complexes 0.5. A Comparison of the Bonding in Np, Pu, and Transplutonium Compounds with That in Lanthanide Compounds and a Transition-Metal Analog. *J. Am. Chem. Soc.* **1991**, *113*, 552−559.
(31) Lukens, W. W.; Andersen, R. A. Synthesis, Structure, and Reactions of $(\eta^5\text{-}C_5H_5)_3Zr$. *Organometallics* **1995**, *14*, 3435−3439.
(32) Denning, R. G.; Harmer, J.; Green, J. C.; Irwin, M. Covalency in the 4f Shell of tris-Cyclopentadienyl Ytterbium ($YbCp_3$)—A Spectroscopic Evaluation. *J. Am. Chem. Soc.* **2011**, *133*, 20644−20660.
(33) Beck, H. P. Notizen: NdI2-II, eine metallisch leitende Hochdruckmodifikation ?/NdI2, a Metallic High Pressure Modification ? *Z. Naturforsch., B: J. Chem. Sci.* **1976**, *31*, 1548.
(34) Gerlitzki, N.; Meyer, G.; Mudring, A.-V.; Corbett, J. D. Praseodymium diiodide, PrI_2, revisited by synthesis, structure determination and theory. *J. Alloys Compd.* **2004**, *380*, 211−218.
(35) Fang, M.; Lee, D. S.; Ziller, J. W.; Doedens, R. J.; Bates, J. E.; Furche, F.; Evans, W. J. Synthesis of the $(N_2)^{3-}$ radical from Y^{2+} and its protonolysis reactivity to form $(N_2H_2)^{2-}$ via the $Y[N(SiMe_3)_2]_3/KC_8$ reduction system. *J. Am. Chem. Soc.* **2011**, *133*, 3784−7.
(36) Zachmanoglou, C. E.; Docrat, A.; Bridgewater, B. M.; Parkin, G.; Brandow, C. G.; Bercaw, J. E.; Jardine, C. N.; Lyall, M.; Green, J. C.; Keister, J. B. The electronic influence of ring substituents and ansa bridges in zirconocene complexes as probed by infrared spectroscopic, electrochemical, and computational studies. *J. Am. Chem. Soc.* **2002**, *124*, 9525−46.
(37) Coles, M. P.; Hitchcock, P. B.; Lappert, M. F.; Protchenko, A. V. Syntheses and Structures of the Crystalline, Highly Crowded 1,3-Bis(trimethylsilyl)cyclopentadienyls $[MCp''_3]$ (M = Y, Er, Yb), $[PbCp''_2]$, $[\{YCp''_2(\mu\text{-}OH)\}_2]$, $[(ScCp''_2)_2(\mu\text{-}\eta^2\text{:}\eta^2\text{-}C_2H_4)]$, $[YbCp''_2Cl(\mu\text{-}Cl)K(18\text{-crown-}6)]$, and $[\{KCp''\}_\infty]$. *Organometallics* **2012**, *31*, 2682−2690.
(38) Peterson, J. K.; MacDonald, M. R.; Ziller, J. W.; Evans, W. J. Synthetic Aspects of $(C_5H_4SiMe_3)_3Ln$ Rare-Earth Chemistry: Formation of $(C_5H_4SiMe_3)_3Lu$ via $[(C_5H_4SiMe_3)_2Ln]^+$ Metallocene Precursors. *Organometallics* **2013**, *32*, 2625−2631.
(39) Woen, D. H.; Chen, G. P.; Ziller, J. W.; Boyle, T. J.; Furche, F.; Evans, W. J. Solution Synthesis, Structure, and CO_2 Reduction Reactivity of a Scandium(II) Complex, $\{Sc[N(SiMe_3)_2]_3\}^{1-}$. *Angew. Chem., Int. Ed.* **2017**, *56*, 2050−2053.
(40) Ryan, A. J.; Darago, L. E.; Balasubramani, S. G.; Chen, G. P.; Ziller, J.; Furche, F.; Evans, W. J. Synthesis, Structure, and Magnetism of Tris(amide) $[Ln\{N(SiMe_3)_2\}_3]^{1-}$ Complexes of the Non-traditional + 2 Lanthanide Ions. *Chem. - Eur. J.* **2018**, *24*, 7702−7709.
(41) In order to support this assignment, the electride species was independently prepared from the reaction of crypt and KC8 in THF. The EPR spectrum of that product gave a signal at g = 2.001, Figure S1. This extra feature was still present even when less than 1 equiv of crypt was used. Consistent with this assignment, the signal became more prominent in the room temperature spectrum possibly because the electride species was more stable than the Y(II) product at this temperature and only a small amount of the Y(II) species survived by the time the spectrum was collected.
(42) Shannon, R. Revised effective ionic radii and systematic studies of interatomic distances in halides and chalcogenides. *Acta Crystallogr., Sect. A: Cryst. Phys., Diffr., Theor. Gen. Crystallogr.* **1976**, *32*, 751−767.
(43) Windorff, C. J.; Dumas, M. T.; Ziller, J. W.; Gaunt, A. J.; Kozimor, S. A.; Evans, W. J. Small-Scale Metal-Based Syntheses of Lanthanide Iodide, Amide, and Cyclopentadienyl Complexes as Analogues for Transuranic Reactions. *Inorg. Chem.* **2017**, *56*, 11981−11989.
(44) Woen, D. H.; Huh, D. N.; Ziller, J. W.; Evans, W. J. Reactivity of Ln(II) Complexes Supported by $(C_5H_4Me)^{1-}$ Ligands with THF and $PhSiH_3$: Isolation of Ring-Opened, Bridging Alkoxyalkyl, Hydride, and Silyl Products. *Organometallics* **2018**, *37*, 3055−3063.
(45) Schumann, H.; Glanz, M.; Hemling, H.; Ekkehard Hahn, F. Metallorganische Verbindungen der Lanthanoide. 93 [1]. Tetramethylcyclopentadienyl-Komplexe ausgewhlter 4f-Elemente. *Z. Anorg. Allg. Chem.* **1995**, *621*, 341−345.
(46) Xie, Z. W.; Chui, K. L.; Liu, Z. X.; Xue, F.; Zhang, Z. Y.; Mak, T. C. W.; Sun, J. Systematic studies on the reactions of lanthanide trichlorides with Na[1,3-bis(trimethylsilyl)cyclopentadienyl]. Crystal structures of $[1,3\text{-}(Me_3Si)_2C_5H_3]_3Ln$ (Ln = La, Nd, Gd, Dy). *J. Organomet. Chem.* **1997**, *549*, 239−244.
(47) Evans, W. J.; Rego, D. B.; Ziller, J. W. Synthesis, structure, and ^{15}N NMR studies of paramagnetic lanthanide complexes obtained by reduction of dinitrogen. *Inorg. Chem.* **2006**, *45*, 10790−8.
(48) Stults, S. D.; Andersen, R. A.; Zalkin, A. Structural Studies on Cyclopentadienyl Compounds of Trivalent Cerium - Tetrameric $(Me_5H_4)_3Ce$ and Monomeric $(Me_3SiC_5H_4)_3Ce$ and $[(Me_3Si)_2C_5H_3]_3Ce$ and Their Coordination Chemistry. *Organometallics* **1990**, *9*, 115−122.
(49) Minasian, S. G.; Krinsky, J. L.; Rinehart, J. D.; Copping, R.; Tyliszczak, T.; Janousch, M.; Shuh, D. K.; Arnold, J. A comparison of 4f vs 5f metal-metal bonds in $(CpSiMe_3)_3M\text{-}ECp^*$ (M = Nd, U; E = Al, Ga; Cp* = C_5Me_5): synthesis, thermodynamics, magnetism, and electronic structure. *J. Am. Chem. Soc.* **2009**, *131*, 13767−83.
(50) Lappert, M. F.; Singh, A.; Atwood, J. L.; Hunter, W. E. Use of the bis(trimethylsilyl)cyclopentadienyl ligand for stabilising early (f^0−f^3) lanthanocene chlorides; X-ray structure of $[(Pr\{\eta\text{-}[C_5H_3(SiMe_3)_2]\}_2Cl)_2]$ and of isoleptic scandium and ytterbium complexes. *J. Chem. Soc., Chem. Commun.* **1981**, *0*, 1190−1191.
(51) Evans, D. F. 400. The determination of the paramagnetic susceptibility of substances in solution by nuclear magnetic resonance. *J. Chem. Soc.* **1959**, 2003−2005.
(52) Becconsall, J. K. Effect of magnetically anisotropic solvent molecules on nuclear screening. *Mol. Phys.* **1968**, *15*, 129−139.
(53) Schubert, E. M. Utilizing the Evans method with a superconducting NMR spectrometer in the undergraduate laboratory. *J. Chem. Educ.* **1992**, *69*, 62.
(54) Weigend, F.; Ahlrichs, R. Balanced basis sets of split valence, triple zeta valence and quadruple zeta valence quality for H to Rn: Design and assessment of accuracy. *Phys. Chem. Chem. Phys.* **2005**, *7*, 3297−3305.
(55) Dolg, M.; Stoll, H.; Savin, A.; Preuss, H. Energy-adjusted pseudopotentials for the rare earth elements. *Theoretica chimica acta* **1989**, *75*, 173−194.

DOI: 10.1021/acs.organomet.8b00557
Organometallics 2018, 37, 3863−3873

(56) Gulde, R.; Pollak, P.; Weigend, F. Error-Balanced Segmented Contracted Basis Sets of Double-ζ to Quadruple-ζ Valence Quality for the Lanthanides. *J. Chem. Theory Comput.* **2012**, *8*, 4062−4068.
(57) Dorenbos, P. f → d transition energies of divalent lanthanides in inorganic compounds. *J. Phys.: Condens. Matter* **2003**, *15*, 575.
(58) Bergbreiter, D. E.; Killough, J. M. Reactions of potassium-graphite. *J. Am. Chem. Soc.* **1978**, *100*, 2126−2134.
(59) Soller, B. S.; Sun, Q.; Salzinger, S.; Jandl, C.; Pöthig, A.; Rieger, B. Ligand Induced Steric Crowding in Rare Earth Metal-Mediated Group Transfer Polymerization of Vinylphosphonates: Does Enthalpy Matter? *Macromolecules* **2016**, *49*, 1582−1589.
(60) Shestakov, B. G.; Mahrova, T. V.; Larionova, J.; Long, J.; Cherkasov, A. V.; Fukin, G. K.; Lyssenko, K. A.; Scherer, W.; Hauf, C.; Magdesieva, T. V.; Levitskiy, O. A.; Trifonov, A. A. Ytterbium(III) Complexes Coordinated by Dianionic 1,4-Diazabutadiene Ligands. *Organometallics* **2015**, *34*, 1177−1185.
(61) Evans, W. J.; Lee, D. S.; Johnston, M. A.; Ziller, J. W. The Elusive $(C_5Me_4H)_3Lu$: Its Synthesis and $LnZ_3/K/N_2$ Reactivity. *Organometallics* **2005**, *24*, 6393−6397.
(62) Goodwin, C. A. P.; Joslin, K. C.; Lockyer, S. J.; Formanuik, A.; Morris, G. A.; Ortu, F.; Vitorica-Yrezabal, I. J.; Mills, D. P. Homoleptic Trigonal Planar Lanthanide Complexes Stabilized by Superbulky Silylamide Ligands. *Organometallics* **2015**, *34*, 2314−2325.
(63) Chilton, N. F.; Goodwin, C. A. P.; Mills, D. P.; Winpenny, R. E. P. The first near-linear bis(amide) f-block complex: a blueprint for a high temperature single molecule magnet. *Chem. Commun.* **2015**, *51*, 101−103.
(64) Goodwin, C. A. P.; Chilton, N. F.; Vettese, G. F.; Moreno Pineda, E.; Crowe, I. F.; Ziller, J. W.; Winpenny, R. E. P.; Evans, W. J.; Mills, D. P. Physicochemical Properties of Near-Linear Lanthanide(II) Bis(silylamide) Complexes (Ln = Sm, Eu, Tm, Yb). *Inorg. Chem.* **2016**, *55*, 10057−10067.

DOI: 10.1021/acs.organomet.8b00557
Organometallics 2018, 37, 3863−3873